

## PDF hosted at the Radboud Repository of the Radboud University Nijmegen

The following full text is a publisher's version.

For additional information about this publication click this link.

<http://hdl.handle.net/2066/98955>

Please be advised that this information was generated on 2021-03-03 and may be subject to change.

# Evidence for orientational tunneling of CO intercalated in C<sub>60</sub>: A nuclear magnetic resonance study

M. Tomaselli<sup>a)</sup> and D. W. Knecht

Laboratory of Physical Chemistry, ETH-Zürich, CH-8092 Zürich, Switzerland

I. Holleman

Department of Molecular and Laser Physics, University of Nijmegen, Toernooiveld I, NL-6525 ED Nijmegen, The Netherlands

G. Meijer

FOM-Institute for Plasma-Physics Rijnhuizen, Postbox 1207, 3430 BE Nieuwegein, The Netherlands and Department of Molecular and Laser Physics, University of Nijmegen, Toernooiveld I, NL-6525 ED Nijmegen, The Netherlands

B. H. Meier

Laboratory of Physical Chemistry, ETH-Zürich, CH-8092 Zürich, Switzerland

(Received 3 May 2000; accepted 2 August 2000)

We characterize the low-temperature dynamics of CO intercalated in C<sub>60</sub> using NMR spectroscopy. CO in C<sub>60</sub> is found to be dynamically inhomogeneous below 30 K: The <sup>13</sup>C line shapes reflect a dynamic disorder to static disorder transition, with only quantum tunneling among equivalent orientations in a local S<sub>6</sub> symmetry potential remaining. The increased hindrance of the CO motion cannot be reconciled with common expectations of a homogeneous, thermally activated jumplike reorientation process, but is well accounted for in a model of orientational pinning due to asymmetric distortions of the cage potential. © 2000 American Institute of Physics.

[S0021-9606(00)70837-3]

It has recently been shown that solid C<sub>60</sub> can be intercalated with CO molecules occupying exclusively the octahedral voids of the cubic closed packed lattice.<sup>1</sup> CO trapped in solid C<sub>60</sub> shows many of the ideal properties anticipated for the corresponding endohedral C<sub>60</sub> species.<sup>2</sup> With a van der Waals length of ~4.4 Å CO fits exactly in the octahedral sites of the C<sub>60</sub> crystal and behaves as an isolated molecule or stick in a box. As such, it forms a model system for the study of virtually free rovibrational motion in the condensed phase.<sup>1,3,4</sup> Due to its special position in the crystal lattice, CO is a sensitive spy to monitor changes in site symmetry imposed by the phase transitions of the C<sub>60</sub> matrix.<sup>1,4-7</sup> Furthermore, it could be envisioned that the trapped CO molecules form the building blocks of an ideal electric dipolar lattice.<sup>8</sup>

In this communication, we emphasize on the rovibrational dynamics of CO in C<sub>60</sub> for temperatures between 3.8 and 30 K using <sup>13</sup>C NMR. New data with higher precision show that the hindered CO motion cannot be described in terms of thermally activated jumplike reorientations as previously proposed.<sup>9</sup> Instead, asymmetric distortions of the local S<sub>6</sub> cage potential induce a pinning for the majority of the trapped CO molecules. Interestingly, a highly delocalized CO fraction persists to the lowest investigated temperatures and is attributed to CO undergoing quantum tunneling between equivalent orientations in an unperturbed or weakly perturbed S<sub>6</sub> potential.

In order to introduce the CO cavity potential and characterize our sample we present also the spectra in the high-temperature regime. Figure 1 shows one-dimensional (1D) NMR spectra of <sup>13</sup>CO (99% <sup>13</sup>C enriched) intercalated in C<sub>60</sub>

(ratio 0.52:1; C<sub>60</sub> purity ≥99.9%) above the glass transition temperature ( $T_g \sim 80$  K).<sup>5</sup> The ~300 mg powder sample was prepared as described previously<sup>1,9</sup> and stored at 180 K. The spectra were acquired at 55.31 MHz (5.17 T field) using a home-built spectrometer and home-built low-temperature probe fitted into a helium cryostat (Oxford Instruments). A typical  $\pi/2$  pulse length of 7  $\mu$ s was used. The sample temperature was measured with a calibrated Cernox resistor (Lake Shore). The motionally narrowed <sup>13</sup>CO spectra in Fig. 1 reveal the change in the local potential symmetry from  $O_h \rightarrow S_6$  when crossing the C<sub>60</sub> orientational ordering transition at ~240 K (fcc  $\rightarrow$  sc).<sup>6</sup> The cage potential is determined by CO-C<sub>60</sub> van der Waals interactions and its characteristics are depicted on the right-hand side of Fig. 1: eight discrete minima orientations of the internuclear CO axis are aligned with the cube diagonals of the C<sub>60</sub> unit cell. The degeneracy of these CO positions ( $O_h$ , fcc) is lifted in the low-temperature C<sub>60</sub> ratcheting phase (S<sub>6</sub>, sc) where the C<sub>60</sub> molecules are inequivalent (defined as  $p$  and  $h$  C<sub>60</sub> orientations).<sup>7</sup> Therefore, two local CO minima orientations along the unique C<sub>3</sub> axis (denoted **B**-type) and six global minima orientations along the remaining cube diagonals (**A**-type) result.<sup>5</sup> The corresponding energy difference  $\Delta E(T)$  between the two types of CO orientations can be extracted from the experimental line shapes (see Fig. 1). Since for  $T > 30$  K, CO reorientations among all minima positions are rapid on the NMR time scale (i.e.,  $\tau_r \ll 1/\Delta\nu = 1/|\nu_{11} - \nu_{33}|$ ), the resulting averaged <sup>13</sup>CO shift anisotropy below 240 K is caused by a mere depopulation of the **B** sites according to the Boltzmann statistics:  $p_B/p_A = 1/3 \exp(-\Delta E/kT)$ . In contrast, the CO rattling motion above 240 K causes the <sup>13</sup>C CSA to collapse to the isotropic

<sup>a)</sup>Electronic mail: mato@nmr.phys.chem.ethz.ch

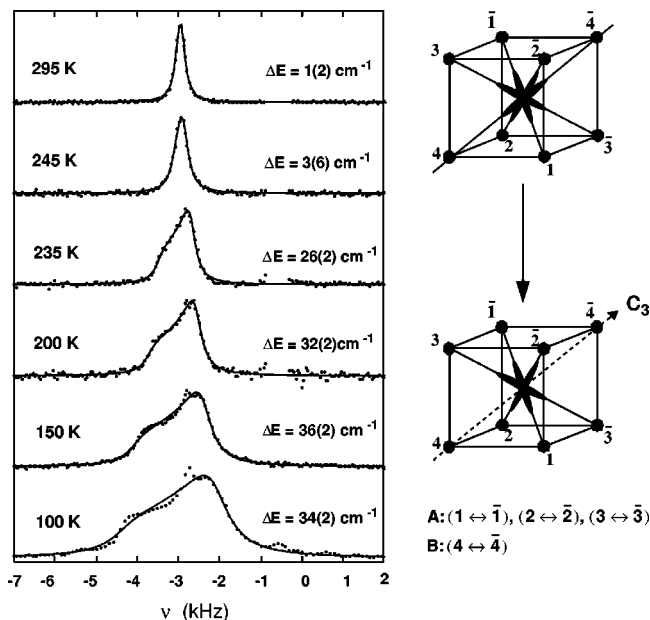


FIG. 1. (a) Experimental (dots) and fitted (lines)  $^{13}\text{CO}$  spectra of  $(\text{CO})_{0.52}\text{C}_{60}$  for  $T > T_g$  (10 s delay between scans; 100 transients). The  $^{13}\text{C}_{60}$  resonance is suppressed in all spectra. Fits are based on a model of fast chemical exchange among the CO minima orientations depicted in the figure and using  $\Delta E$  (see main text) as the only nontrivial fit parameter. It is assumed that CO can only jump between neighboring minima, i.e., via the edges of the cube shown above, with a correlation time  $\tau_r$  ( $\text{A} \leftrightarrow \text{A}$ ,  $\text{B} \rightarrow \text{A}$ ) or  $\tau_r' = \tau_r \exp(\Delta E/kT)$  ( $\text{A} \rightarrow \text{B}$ ). The  $^{13}\text{CO}$  chemical shift anisotropy (CSA) was measured independently at 4 K in pure  $\alpha$ -CO [principal values  $(\delta_{11}, \delta_{22}, \delta_{33}) = (310, 310, -73)$ , in ppm relative to tetramethylsilane].

value due to the  $O_h$  symmetry of the cage in the fcc phase. Below  $T_g \sim 80$  K  $(\text{CO})_{0.52}\text{C}_{60}$  forms an orientational glass. The  $\text{C}_{60}$  molecules are frozen in either the  $p$  or  $h$  orientation in a ratio  $\sim 12.5:1^5$  (compare with the ratio of 5:1 in pristine  $\text{C}_{60}$ ).<sup>7</sup> In the glass phase only a fraction of CO sites retains local  $S_6$  symmetry (with all surrounding  $\text{C}_{60}$  molecules being in the energetically preferred  $p$  orientation): i.e.,  $\sim 63\%$  if CO van der Waals interactions with the six nearest  $\text{C}_{60}$  spheres are taken into account, and only  $\sim 34\%$  if nearest and next-nearest neighbors (fourteen  $\text{C}_{60}$  molecules) are considered. The potential symmetry of the remaining CO sites is lowered or lost ( $C_1$ ).

Experimental (dots) and fitted (lines)  $^{13}\text{C}$  single-pulse spectra of  $(\text{CO})_{0.52}\text{C}_{60}$  for  $T < T_g$  are displayed in Fig. 2(a). Contrary to the spectra shown in Fig. 1, the  $^{13}\text{C}_{60}$  matrix resonance is overlapping with the  $^{13}\text{CO}$  resonance and it has to be explicitly taken into account in the analysis. No differences in the experimental line shapes were found when the spectra were acquired with a  $(\pi/2)-\tau-(\pi)-\tau$  Hahn-echo excitation sequence ( $\tau = 300 \mu\text{s}$ , data not shown). This indicates that the spectra are inhomogeneously broadened at all temperatures and CO or  $\text{C}_{60}$  components with reorientational correlation times in the range  $\tau_c \sim 1/\Delta\nu$  are absent. It should also be noticed that in this temperature regime the spin-lattice relaxation time  $T_1$  of both,  $^{13}\text{C}_{60}$  and  $^{13}\text{CO}$ , resonances is highly anisotropic and a repetition delay of  $t_{\text{rep}} = 3$  h between successive experiments was necessary to obtain fully relaxed, undistorted 1D spectra. From Fig. 2(a) it is evident that the  $^{13}\text{C}_{60}$  resonance shows a well defined CSA powder pattern at all temperatures [ $(\delta_{11}, \delta_{22}, \delta_{33})$

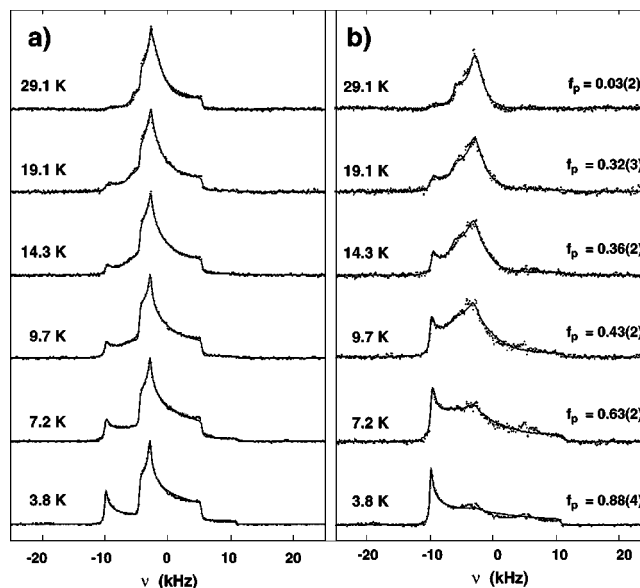


FIG. 2. (a) Single-pulse  $^{13}\text{C}$  spectra of  $(\text{CO})_{0.52}\text{C}_{60}$  for  $T < 30$  K: 3 h delay between scans; eight transients (dotted lines: experiments, solid lines: least-squares fits described in the main text). The data combine experiments taken both on heating and on cooling. No hysteresis was observed. (b) Only the renormalized  $^{13}\text{CO}$  contributions of the spectra in (a) are shown (dotted lines: experiments with the  $^{13}\text{C}_{60}$  resonance subtracted, solid lines: least-squares fits).

$= (214, 183, 32)$  ppm], implying that below 30 K the  $\text{C}_{60}$  ratcheting motion is indeed completely blocked on the nuclear magnetic resonance (NMR) time scale. The details of the  $^{13}\text{CO}$  line are better visible in Fig. 2(b) where the fitted  $^{13}\text{C}_{60}$  resonance is subtracted. The temperature-dependent line shape can be described quite well with a superposition of two different  $^{13}\text{CO}$  CSA powder patterns: (1) a localized  $^{13}\text{CO}$  component exhibiting the full shift anisotropy [ $(\delta_{11}, \delta_{22}, \delta_{33}) = (312, 312, -71)$  ppm] and (2) a delocalized  $^{13}\text{CO}$  component showing the characteristic inverted sign of its averaged anisotropy compared to that of solid  $^{13}\text{CO}$  (similar to the high-temperature behavior). Upon lowering the temperature, the motionally averaged  $^{13}\text{CO}$  CSA feature broadens with a concomitant decrease in integrated intensity. Conversely, the localized CO fraction continuously gains in intensity; its fitted relative amplitude  $f_p(T)$  is indicated on the right side of Fig. 2(b). At the lowest investigated temperature  $f_p \sim 0.88$ , and therefore the majority of CO sites has lost local  $S_6$  potential symmetry. The experimental data in Fig. 2 imply a *dynamic disorder to static disorder transition via pinning* for most of the CO molecules below 30 K. This is tantamount to a sudden blocking of the reorientational CO motion leading to dynamical inhomogeneity. The present result is clearly at odds with an interpretation of the hindered CO dynamics in terms of a homogeneous, thermally activated reorientation process with  $\tau_r \geq 1/\Delta\nu$ .<sup>9</sup>

In the fits of Figs. 2(a) and 2(b) theoretical CSA patterns for the  $^{13}\text{C}_{60}$  and pinned  $^{13}\text{CO}$  components are used, while for the delocalized  $^{13}\text{CO}$  fraction the experimental line shapes as shown in Fig. 3(a) serve as the third input parameter [two nontrivial intensity fitting parameters in total:  $f_{de}$  (delocalized CO) and  $f_p$  (pinned CO);  $f_{\text{C}_{60}} = 1 - f_{de} - f_p$ ]. The  $^{13}\text{C}$  line shapes from delocalized CO components can be

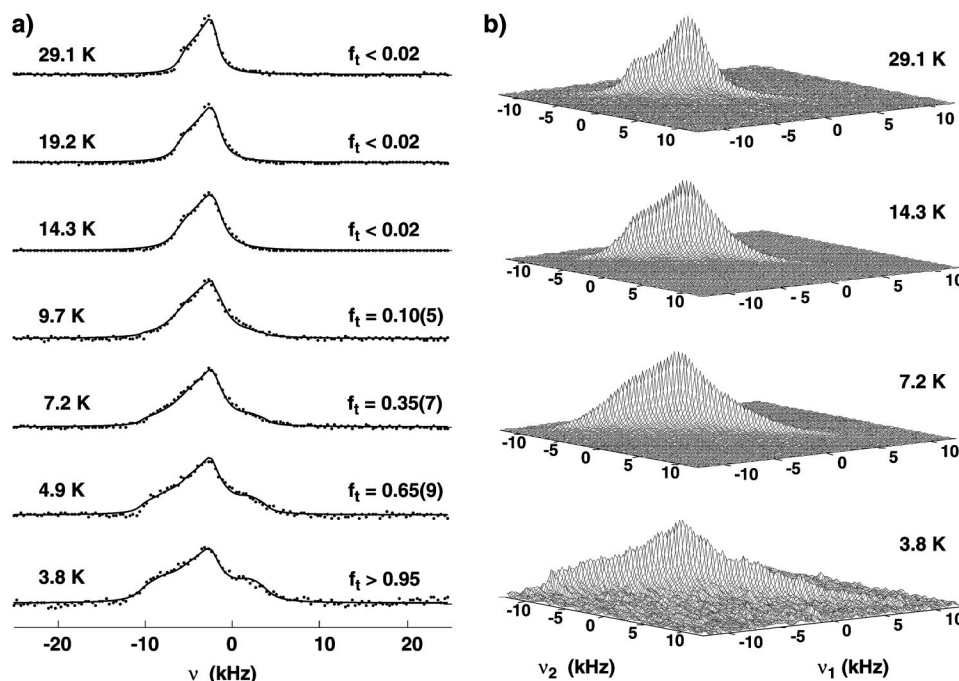


FIG. 3. (a) SAT- $\tau_d$ - $(\pi/2)$ DET  $^{13}\text{C}$  spectra of  $(\text{CO})_{0.52}\text{C}_{60}$  for  $T < 30$  K: 4 s delay between scans; 6144 transients (dotted lines: experiments, solid lines: least-squares fits described in the main text). (b)  $^{13}\text{C}$  2D exchange spectra of  $(\text{CO})_{0.52}\text{C}_{60}$  with a presaturation delay  $\tau_d = 200$  ms. 4 s delay between scans; 512 transients per  $t_1$  value. An exchange time  $\tau_e = 100$  ms ( $\gg 1/\Delta\nu$ ) was used at all temperatures.

resolved directly by taking advantage of the large differences in  $T_1$  between the sites. We found that below 30 K these sites reach their maximum signal amplitude already for  $t_{\text{rep}} \sim 10$  s, while the other two components ( $^{13}\text{C}_{60}$  and pinned  $^{13}\text{CO}$ ) have much longer  $T_1$  and still increase in intensity for  $t_{\text{rep}} > 1$  h. It is surmised that the dominant relaxation mechanism for  $^{13}\text{C}_{60}$  and pinned  $^{13}\text{CO}$  is provided by spin diffusion with dynamic  $^{13}\text{CO}$  entities.<sup>10</sup> This mechanism also explains the above-mentioned anisotropy in  $T_1$ . The spectra displayed in Fig. 3(a) were obtained with the timing sequence SAT- $\tau_d$ - $(\pi/2)$ DET, where SAT denotes a train of 20  $\pi/2$  pulses separated by 20 ms that saturates (destroys) any  $^{13}\text{C}$  polarization. During  $\tau_d = 200$  ms part of the  $^{13}\text{C}$  polarization from delocalized CO sites rebuilds, and DET represents the detection of the free induction decay following a single  $\pi/2$  pulse. No differences in the line shapes were found when SAT was altered to 100  $\pi/2$  pulses separated by 4 ms and  $\tau_d$  varied between 30 and 300 ms.  $^{13}\text{C}$  probe-background signals were not observed in our setup and checked by running identical measurements without the sample present. For  $T > 10$  K the line shapes in Fig. 3(a) clearly show the signature of dynamic  $^{13}\text{CO}$  sites with  $\tau_r \ll 1/\Delta\nu$  in an environment with effective  $S_6$  symmetry (see Fig. 1). The slight broadening of the averaged CSA tensor at 14.3 and 19.2 K compared to 29.1 K can be attributed to a complete depopulation of the **B** orientations in accordance with expectations for an energy splitting of  $\Delta E \sim 36 \text{ cm}^{-1}$  and following the Boltzmann statistics (see Fig. 1). The exchange-model fits in this temperature range give a slightly different CO orientational geometry than the one depicted in Fig. 1. It is found indeed that the tetrahedral angle ( $109.47^\circ$ ) between the **A**- and **B**-type orientations for cubic geometry increases by  $7 \pm 2^\circ$ . This results in a slight misalignment of the CO axes with the  $(1, \pm 1, \pm 1)$  directions of the  $\text{C}_{60}$  unit cell, but still retains the

local  $S_6$  potential symmetry and degeneracy of the **A** orientations if all angles  $\angle_{\text{AB}}$  are equally affected. It should be noticed, however, that according to Fig. 2(b) the condition of roughly degenerate **A** orientations is only fulfilled for  $\sim 60\%$  of all CO sites at 10 K. Indications for a distortion of the CO axes geometry upon crossing the glass transition were also found by x-ray diffraction.<sup>5</sup>

Below 10 K the  $^{13}\text{CO}$  line changes shape. Around 4–5 K it cannot be described by the classical model of Fig. 1 anymore (even with the inclusion of potential asymmetries among **A** orientations with  $\Delta E_A \leq kT$ ). Instead, the spectrum at 3.8 K is well approximated by a model of coherent tunnel motion of  $^{13}\text{CO}$  between the six equivalent **A** orientations in a  $S_6$  potential well. In the quantum-mechanical approach we include, in analogy to the classical model, only tunnel matrix elements between neighboring **A** orientations. This results in a fourfold splitting of the CO ground librational level as  $A_g - E_u - E_g - A_u$  (in order of increasing energy).  $A$  and  $E$  levels split by the tunnel-energy  $\Delta E_t$ , whereas the two  $E$  levels are separated by  $2\Delta E_t$ . The tunnel spectrum of  $^{13}\text{CO}$  in its librational ground state is then calculated in the limit  $\Delta E_t/h = \nu_t \gg \Delta\nu$ . Our assumptions are supported by theoretical calculations of the  $(\text{CO})\text{C}_{60}$  cavity potential (ideal  $S_6$  symmetry, with all surrounding  $\text{C}_{60}$  molecules in the  $p$  orientation) where a tunnel splitting of  $\Delta E_t \sim 0.6 \text{ cm}^{-1}$  and  $\Delta E^{1,2} \sim 32 \text{ cm}^{-1}$  for the first fundamental van der Waals mode are predicted<sup>4</sup> (i.e., a population of excited librational states is negligible below 10 K). In accordance with the results at  $10 < T < 30$  K we find  $\angle_{\text{AB}} \sim 118^\circ$ , i.e., a deviation of  $9 \pm 2^\circ$  from the tetrahedral CO-axes arrangement must be included in the model to fit the experimental spectrum at 3.8 K.

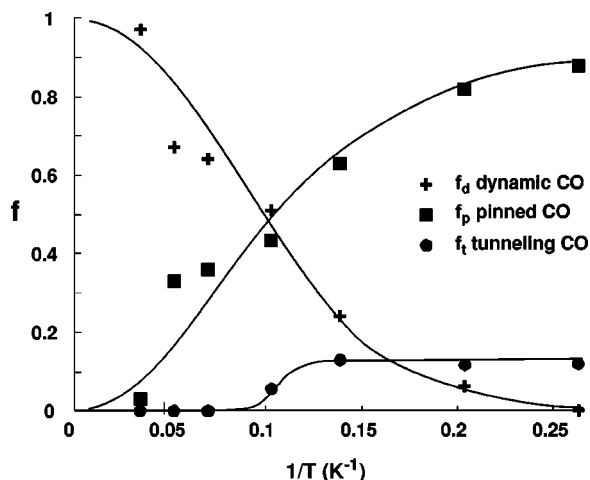


FIG. 4. Graph of  $f_p$ ,  $f_d$ ,  $f_t$  vs  $1/T$ , monitoring the dynamic to static disorder transition below 30 K and the emergence of exchange tunneling below  $\sim 10$  K. The solid lines are meant to guide the eye.

Additional two-dimensional (2D) NMR experiments<sup>11</sup> were performed to aid in the interpretation of the line shapes displayed in Fig. 3(a). We acquired 2D exchange data using the pulse sequence SAT- $\tau_d$ - $(\pi/2)_{\phi_1}$ - $t_1$ - $(\pi/2)_{\phi_2}$ - $\tau_e$ - $(\pi/2)_{\phi_3}$ - $t_2$  (DET), with phase cycling  $\phi_1, \phi_2, \phi_3$  to suppress artifacts. The exchange and presaturation periods ( $\tau_e, \tau_d$ ) were kept fixed and  $t_1$  was incremented from 1 to 3000  $\mu$ s. Fourier transformation of the signal  $S(t_1, t_2; \tau_e)$  yields the 2D spectrum  $F(\nu_1, \nu_2; \tau_e)$  which indicates correlations of  $^{13}\text{C}$  frequencies before ( $\nu_1$ ) and after ( $\nu_2$ ) the exchange period. Representative 2D spectra are shown in Fig. 3(b). By setting  $\tau_d = 200$  ms the delocalized  $^{13}\text{C}$  fraction was selectively excited. It is clearly seen that the total spectral intensity in the 2D data lies always along the diagonal ( $\nu_1 = \nu_2$ ), implying that the delocalized  $^{13}\text{C}$  line is indeed inhomogeneously broadened at all temperatures. No indication for exchange broadening is found. This corroborates our interpretation of the experimental data above 10 K [Fig. 3(a)] in terms of motionally narrowed  $^{13}\text{C}$  line shapes with  $\tau_r \ll 1/\Delta\nu$ . In addition, it becomes clear that the observed broadening and change of line shape below 10 K cannot be attributed to incoherent exchange processes with correlation times  $\tau_r \geq 1/\Delta\nu$  (i.e., the onset of motional narrowing). This precludes an interpretation of the spectra according to energy-activated incoherent tunneling processes, as often found for methyl rotors.<sup>12</sup> Instead, we can describe the experimental data as a superposition of delocalized  $^{13}\text{C}$  sites performing incoherent jumps among the A orientations with  $\tau_r \ll 1/\Delta\nu$  and a second fraction of delocalized  $^{13}\text{C}$  sites emerging below  $\sim 10$  K and undergoing tunneling between equivalent A orientations. The fitted relative amplitude of the tunneling  $^{13}\text{C}$  fraction  $f_t(T)$  is given on the right-hand side of Fig. 3(a). This model clearly fulfills the constraints imposed by the 2D exchange spectra shown in Fig. 3(b). The results are summarized in Fig. 4, where the relative intensities of the various CO sites are shown as a function of  $1/T$ . The graph indicates a transition from a situation in which all CO molecules have significant freedom to move to a situation in which the motion is completely blocked, with only tunneling remaining for a subfraction below  $\sim 10$  K. It is concluded that the potential symmetry for tunneling CO sites

is still approximately  $S_6$  with  $\Delta E_A \ll \Delta E_t \sim 0.6 \text{ cm}^{-1}$ , as estimated from theoretical calculations.<sup>4</sup> For the majority of the sites, however, the  $S_6$  symmetry is broken ( $\Delta E_A > 3 \text{ cm}^{-1} \sim kT$  at 4 K), and the CO molecules localize in one of the minima of the potential well. This interpretation is substantiated by 2D exchange experiments recorded at 25, 14.3, 4.9, and 3.8 K with  $\tau_d = 80$  s and  $\tau_e = 10$  s, where the pinned  $^{13}\text{C}$  sites are selectively observed<sup>13</sup> (data not shown). The absence of any off-diagonal signals in these 2D spectra implies that for  $T < 30$  K no large amplitude CO reorientations occur even over a time period of 10 s.

It is interesting to relate the present NMR results for  $(^{13}\text{C})_{0.52}\text{C}_{60}$  with recent infrared (IR) absorption experiments performed on  $(^{12}\text{C}^{16}\text{O})_{-1}\text{C}_{60}$ .<sup>4</sup> From a splitting of the fundamental IR transition below 10 K into two components separated by  $0.9 \text{ cm}^{-1}$  (intensity ratio:  $\sim 1:3$ ) it was concluded that CO is present in at least two different octahedral cavities. Furthermore, a splitting of the IR resonance due to a tunneling of CO, if at all present, is less than  $\sim 0.4 \text{ cm}^{-1}$ .<sup>4</sup> These findings are not in contradiction with our NMR results. It is remarkable that the inhomogeneous character of  $(\text{CO})\text{C}_{60}$  below 30 K is reflected by both techniques, although the detected heterogeneities can be of different nature due to the vastly different time scales probed by the two experiments, and due to the much higher CO intercalation ratio for the samples studied by IR.<sup>1</sup>

The cause for the observed pinning of CO in  $\text{C}_{60}$  (in contrast to a continuous localization) is not well understood at present. It can be speculated that cooperative effects, due to interactions between partially screened CO dipoles in regions with high intercalation densities,<sup>8</sup> give rise to this behavior, and as such, indicates a phase transition (possibly with the formation of domains) below 30 K. This might also explain the unusual transition to the tunnel regime for part of the CO sites reflected in Figs. 3 and 4. More experiments, in particular  $(^{17}\text{O})\text{C}_{60}$  line shape and  $T_1$  relaxation studies, are needed to clarify the relative influences of the static structural disorder and the cooperative behavior.

We thank G. von Helden and R. Meyer for useful advice and experimental assistance.

<sup>1</sup>I. Holleman *et al.*, Phys. Rev. Lett. **79**, 1138 (1997).

<sup>2</sup>H.W. Kroto *et al.*, Nature (London) **318**, 162 (1985); M. Saunders *et al.*, *ibid.* **367**, 256 (1994); N. Weiden, H. Käss, and K.-P. Dinse, J. Phys. Chem. B **103**, 9826 (1999); E.H.T. Olthof, A. van der Avoird, and P.E.S. Wormer, J. Chem. Phys. **104**, 832 (1996).

<sup>3</sup>A.I. Kolesnikov *et al.*, J. Phys.: Condens. Matter **9**, 2831 (1997); B. Morosin *et al.*, Phys. Rev. B **57**, 13611 (1997); S.A. FitzGerald *et al.*, *ibid.* **60**, 6439 (1999).

<sup>4</sup>I. Holleman *et al.*, Phys. Rev. Lett. **80**, 4899 (1998); J. Chem. Phys. **110**, 2129 (1999).

<sup>5</sup>S. van Smaalen *et al.*, Phys. Rev. B **57**, 6321 (1998); Europhys. Lett. **43**, 302 (1998).

<sup>6</sup>P.A. Heiney *et al.*, Phys. Rev. Lett. **66**, 2911 (1991); R. Tycko *et al.*, *ibid.* **67**, 1886 (1991).

<sup>7</sup>W.I.F. David *et al.*, Europhys. Lett. **18**, 219 (1992).

<sup>8</sup>J. Cioslowski and A. Nanayakkara, Phys. Rev. Lett. **69**, 2871 (1992).

<sup>9</sup>I. Holleman *et al.*, J. Am. Chem. Soc. **121**, 199 (1999).

<sup>10</sup>N. Bloembergen, Physica (Amsterdam) **15**, 386 (1949).

<sup>11</sup>J. Jeener *et al.*, J. Chem. Phys. **71**, 4546 (1979).

<sup>12</sup>A. Szymański, J. Chem. Phys. **111**, 288 (1999).

<sup>13</sup>The delocalized  $^{13}\text{C}$  sites relax during this mixing time. Within experimental error, identical line shapes as shown in Fig. 3(a) are retrieved in difference spectra with  $\tau_e = 10$  s and  $\tau_d = 0$  ( $\tau_d = 80$  s).